Optical scatterings in layered systems

Chang-Ting Liu
National Kaohsiung Normal University
Chih-Wei Chiu (giorgio@mail.nknu.edu.tw)
National Kaohsiung Normal University
Chiun-Yan Lin
National Cheng Kung University
Ming-Fa Lin
National Cheng Kung University

Research Article

Keywords: optical properties, reflectance, absorbance,transmittance spectra,

Posted Date: December 22nd, 2020

DOI: https://doi.org/10.21203/rs.3.rs-125672/v1

Optical scatterings in layered systems

Chang-Ting Liu,[1] Chih-Wei Chiu,[1] Chiun-Yan Lin[2] and Ming-Fa Lin[2]
[1]Department of Physics, National Kaohsiung Normal University ,Kaohsiung 824, Taiwan
[2]Department of Physics, National Cheng Kung University, Tainan 701, Taiwan

December 10, 2020

Abstract

Optical properties, reflectance, absorbance and transmittance spectra, are fully investigated for the layered structures through the development of theoretical framework. The transverse dielectric function, which characterizes the dynamic charge screenings, can cover all the intralayer and interlayer atomic interactions under the electro-magnetic wave perturbation. By the continuous reflection and transmission scatterings at two surfaces, their analytic formulas are established from the vertical valence-state transitions and the boundary conditions. They are also suitable for finite-width bulk materials. Most important, this study is fully combined with the generalized tight-binding model with all the intrinsic interactions and external field.

Corresponding author : giorgio@mail.nknu.edu.tw(Chih-Wei Chiu)

1 Introduction

Layered graphene systems are one of the main-stream materials [1–3], since they possess various crystal symmetries. The number of layers, stacking configurations and external fields can create the diverse phenomena [3,4], e.g., the easy modulations about the vertical optical transitions. There are a lot of theoretical [4–7] and experimental studies [8–12] on few-layer graphene systems. The main focuses cover the low-frequency absorption structures in the presence/absence of gate voltage and magnetic field. Specially, the magneto-optical theory is developed through the generalized tight-binding model based on two sublattices of each honeycomb crystal. The systematic investigations for the diversified magnetic quantization have been done for 2D materials [4, 5], such as, the unusual Landau levels and magneto-optical selection rules. This theoretical framework is useful in fully understanding the electronic [1, 2], magnetic [5, 8], optical [4–12], transport [13] and Coulomb-excitation [14] properties under the intrinsic atomic interactions and field perturbations. However, the Kubo formula is not enough in exploring reflectance and transmittance spectra of thin films with prominent boundary effects. In this work, an optical scattering model is developed within the previous framework. The calculated results could be examined by the high-resolution optical measurements [8–12].

The π-electronic states of sp^2-bonding systems [1–3] are responsible for the essential properties, such as, graphenes [1, 15], carbon nanotubes [16–18], graphene nanoribbons [19–21], onions [22,23] and fullerenes [24,25]. Very interesting, such carriers dominate the dynamic/static screening responses under the significant perturbation of an electromagnetic/Coulomb field [4, 14], as clearly revealed in rich absorption spectra of few-layer graphene systems [8–10]. The inter-π-band transitions, which correspond to the occupied valence subbands and the unoccupied conduction ones, can absorb photon energies and thus induce an obvious decline of a propagating EM wave. The close relations between charges and fields are well characterized by the transverse dielectric function [26]. $\epsilon(\omega)$ of

a multi-/few-layer graphene system will be evaluated under the generalized tight-binding model [14], being suitable under perpendicular gate voltages and uniform magnetic fields.

In this work, a full optical theory is developed for the 2D layered graphene systems. Their band structures and wave functions are calculated within the generalized tight-binding model in the presence/absence of external fields [4, 14]. They are responsible for the dynamic charge screenings of an electromagnetic field through the evaluated dielectric function at long wavelength limit. The perturbation of an electric dipole moment is calculated by the gradient approximation [4, 5]. By the direct combination of $\epsilon\,(\omega\,)$ and two boundary conditions at the upper and lower surfaces, the whole propagating paths can be characterized by the optical excitation process inside the multi-layer honeycomb lattices and the continuous boundary scatterings of incidence, reflection and refraction. As a result, both reflectance and transmittance are expressed as an analytic formula, covering the useful information about the crystal symmetries [27] and the main feature of electronic properties [4, 27, 28].

2 Theories

The featured optical excitations are directly reflected from the main characteristics of electronic structures. In general, the low-lying electronic energy spectra of layered graphene systems, with $E^{c,v} \leq 3$ eV [4–7], are well characterized by the extended C-$2p_z$ π bondings on each honeycomb lattice. The first-principles calculations would become too cumbersome to deal with the other essential properties for thin film beyond the layer number of one hundred. On the other side, the generalized tight-binding model is suitable for a lot layers and even in perpendicular electric and magnetic fields [4, 5]. For a N_L-layer AB-stacked graphene, the C-$2p_z$-based Hamiltonian, the $2N_L \times 2N_L$ Hermitian matrix,, could

be expressed as

$$H_{l,m} = \begin{cases} \gamma_6 & \text{if } m = l,\ m = 2I+1 \\ \gamma_0 h & \text{if } m = l+1,\ m = 4I+2 \\ \gamma_0 h^* & \text{if } m = l+1,\ m = 4I \\ \gamma_1 & \text{if } m = l+2,\ m = 4I+1\,\&\,4I+3 \\ \gamma_3 h & \text{if } m = l+2,\ m = 4I \\ \gamma_3 h^* & \text{if } m = l+2,\ m = 4I+2 \\ \gamma_4 h & \text{if } m = l+1,\ m = 4I+1; \\ & \quad m = l+3,\ m = 4I+2 \\ \gamma_4 h^* & \text{if } m = l+1,\ m = 4I+3; \\ & \quad m = l+3,\ m = 4I \\ \gamma_5/2 & \text{if } m = l+4,\ m = 2I+1 \\ \gamma_2/2 & \text{if } m = l+4,\ m = 2I \\ 0 & \text{otherwise} \end{cases}, \quad (1)$$

where $h = exp(ik_x b) + cos(k_y\sqrt{3}b/2)exp(-ik_y b/2)$. Figure 1(a) clearly the significant atomic interactions on the same layer [γ_0], for the neighboring/next-neighbor layers [γ_1, γ_3, γ_4/γ_2, γ_5], and through the distinct chemical environments [γ_6] [29]. The similar form is revealed in AAA, ABC and AAB [29–31], but under the quite different interlayer hopping integrals. The diverse band structures are easily modulated by the geometry symmetries, covering the semi-metallic behaviors due to the weak overlaps of valence and conduction subbands [inset in Fig.1(b)], the enhanced asymmetry of valence hole and conduction electron spectra about the Fermi level, and the obvious energy dipersions with band-edge states {the critical points or van Hove singularities; [27]}. Apparently, these features strongly affect the optical excitation responses.

When any condensed-matter system is present in an electromagnetic field, all the charges very efficiently screen the external perturbations by creating the induced current density. Their electronic states are vertically excited from the occupied to unoccupied ones under

the quasiparticle absorption process [32]. That is, a valence electron absorbs one photon becomes an excited conduction one. The electric dipole is responsible for driving all the optical transition channel. By the delicate calculations on its inner products, the imaginary-part dielectric function could be evaluated from the Fermi-golden rule, as expressed in

$$Im[\epsilon(\omega)] = \frac{8\pi e^2}{N_L} \sum_{h,h'} \int_{1stBZ} \frac{d\mathbf{k}}{(2\pi)^2} \frac{\left| \left\langle \Psi_{\mathbf{k}}^{h'} \left| \frac{\hat{\mathbf{E}}\cdot\mathbf{P}}{m_e} \right| \Psi_{\mathbf{k}}^{h} \right\rangle \right|^2}{\omega_{ex}^2(\mathbf{k})} \times \frac{\left[n_F(E^{h'}(\mathbf{k})) - n_F(E^{h}(\mathbf{k})) \right] \delta}{\left[\omega_{ex}(\mathbf{k}) - \omega \right]^2 - \delta^2}. \quad (2)$$

where h (h') represents the initial (final) state, $n_F(E(\mathbf{k}))$ is the Fermi-Dirac distribution function, and δ (=0.01 eV), the energy width due to various deexcitation mechanisms, is treated as a free parameter in the calculations. The excitation energy $\omega_{ex}(\mathbf{k}) = E^{h'}(\mathbf{k}) - E^{h}(\mathbf{k})$ arises from the same and different subbands. Furthermore, the real-part one is further calculated by the Kramers-Kronig relations {the principle-value integrations; [32]}. Equation (2) covers the joint density of states and the velocity matrix elements, respectively, dominating the number of excitation channels and scattering amplitudes {optical selection rules; [4–7]}. The gradient approximation is very convenient and reliable in resolving the second term, e.g., the successful evaluations on graphite intercalation compounds [33], carbon nanotubes [34], and few-layer graphenes [4, 5, 35–37]. This linear Kubo formula, which is directly combined with the generalized model, is successful in exploring the diverse magneto-optical excitations of 2D layered structures, e.g., the systematic investigations on magnetic quantization phenomena of layered group-IV and group-V materials [38].

Very interesting, the significant couplings of carrier charges and electromagnetic waves are rather sensitive to position and time. In general, their dynamic screening and propagating behaviors are dominated by the Helmholtz equation [32]. The linear energy dispersion relation in free space would become a non-linear one of $\epsilon\,(\omega\,)\,\omega^2 = c^2k^2$ in any material. The real- and imaginary-part dielectric function could lead to the reduce of group velocity and the decline of spectrum intensity, mainly owing to the imaginary wave vector through the specific relations $k = [\omega\,/c]N(\omega\,)$ and $N(\omega\,) = \sqrt{\epsilon\,(\omega\,)} = n(\omega\,) + i\kappa(\omega\,)$ [32]. n and κ,

respectively, represent the refractive index and extinction coefficient. The absorption coefficient, $\alpha = [\kappa\,\omega\,/c]^{-1}$, is very useful in understanding the characteristic decay length under the efficient photon absorptions of the valence quasiparticles. Apparently, layered graphene systems provide the effective inter-π-band transitions in the particle-field couplings [Fig. 1(b)], even dominating the continuous scatterings at the upper and lower boundaries. It should be noticed that such π valence electrons absorb the electromagnetic-field energy and then release them to heat reservoir by gradually enhancing temperature. The energy transfer between them is an interesting open issue [39, 40].

An electromagnetic wave with $\mathbf{E_I} = E_{\rm I}\,exp[i(\frac{\omega}{c}\,z - \omega\,t)]\,\hat{x}$ and $\mathbf{B_I} = E_{\rm I}\,exp[i(\frac{\omega}{c}\,z - \omega\,t)]\,\hat{y}$ in a free space [a dielectric constant of ϵ_0] is assumed to be normally incident on the upper surface a finite-width sample, as clearly illustrated in Fig. 2. Electric and magnetic fields behave as

$$\begin{aligned}
&\mathbf{E_{R},}_j = E_{{\rm R},j}\,exp[i(-\tfrac{\omega}{c}\,z - \omega\,t)]\,\hat{x} \quad \& \\
&\mathbf{B_{R},}_j = -E_{{\rm R},j}\,exp[i(-\tfrac{\omega}{c}\,z - \omega\,t)]\,\hat{y} \qquad\qquad \text{for } \; z < 0, \\
&\\
&\mathbf{E}_j = E_j\,exp\{i[(-1)^{j-1}\tfrac{\omega}{c}\,Nz - \omega\,t]\}\,\hat{x} \quad \& \\
&\mathbf{B}_j = (-1)^{j-1}E_j\,exp\{i[(-1)^{j-1}\tfrac{\omega}{c}\,Nz - \omega\,t]\}\,\hat{y} \qquad \text{for } \; 0 < z < d, \\
&\\
&\mathbf{E_{T},}_j = E_{{\rm T},j}\,exp[i(\tfrac{\omega}{c}\,z - \omega\,t)]\,\hat{x} \quad \& \\
&\mathbf{B_{T},}_j = E_{{\rm T},j}\,exp[i(\tfrac{\omega}{c}\,z - \omega\,t)]\,\hat{y} \qquad\qquad \text{for } \; z > d.
\end{aligned} \tag{3}$$

Its propagation experiences the first incidence, reflection and transmission, indicating the significant coupling of fields and charges. Obviously, this scattering event is mainly determined by two independent boundary conditions, namely, the continuities of tangential

electric and magnetic fields

$$\begin{aligned} &E_{\rm I} + \textstyle\sum_j^{m+1} E_{{\rm R},j} = \sum_j^{2m} E_j \quad \& \\ &E_{\rm I} - \textstyle\sum_j^{m+1} E_{{\rm R},j} = N \sum_j^{2m} (-1)^{j-1} E_j \qquad\qquad \text{at} \quad z = 0, \end{aligned} \tag{4}$$

$$\begin{aligned} &\textstyle\sum_j^{2m} E_j \, exp[(-1)^{j-1} i \frac{\omega}{c} N d\,] = exp[i \frac{\omega}{c} d\,] \sum_j^m E_{{\rm T},j} \quad \& \\ &N \textstyle\sum_j^{2m} (-1)^{j-1} E_j \, exp[(-1)^{j-1} i \frac{\omega}{c} N d\,] = exp[i \frac{\omega}{c} d\,] \sum_j^m E_{{\rm T},j} \ \text{ at } \quad z = d. \end{aligned}$$

The transmitted wave will propagate along the z-direction, but with the declines intensity by the Landau damping of the inter-π-band excitations [32]. After reaching the opposite surface, the similar scattering behavior come to exist there. Part of wave can penetrate into the outside environment and then make certain contribution to the transmitted field. The others are directly reflected and continue their interactions with the whole valence charges. With the next scattering at the initial surface, the second contribution to the reflected field is achieved through the same boundary conditions. A series of reflections and transmissions, which, respectively, occur at the upper and lower surfaces, could be analytically calculated and expressed as

$$\frac{\sum_j^{m+1} E_{{\rm R},j}}{E_{\rm I}} = \frac{[1 - N^2(\omega)][1 - e^{i2N(\omega)\frac{\omega}{c}d}]}{[1 + N(\omega)]^2 - [1 - N(\omega)]^2 e^{i2N(\omega)\frac{\omega}{c}d}}, \tag{5}$$

$$\&$$

$$\frac{\sum_j^{m} E_{{\rm T},j}}{E_{\rm I}} = \frac{4N(\omega) e^{-i[1-N(\omega)]\frac{\omega}{c}d}}{[1 + N(\omega)]^2 - [1 - N(\omega)]^2 e^{i2N(\omega)\frac{\omega}{c}d}} \tag{6}$$

The total electric fields of the reflected [Eq. (5)] and transmitted [Eq. (6)] electromagnetic waves are very sensitive to the dielectric function and sample width [d]. Their squares are the frequency-dependent reflectance and transmittance spectra [$R(\omega)$ and $T(\omega)$], being directly examined by the optical measurements [8–12].

3 Results

The quantum-confinement effects of optical excitations are clearly shown in layered graphene systems with AB stackings. Reflectance and transmittance, being indicated in Figs. 3(a)

and 3(b), respectively, present the strong frequency- and layer-dependences. Very interesting, the π-electronic excitations have created the prominent vertical transitions at the low and middle frequency ranges. That is, two and three prominent absorption structures come to exist at $\sim 0.10 - 0.81$ eV and $\sim 4.7 - 5.6$ eV, respectively. The former and the latter mainly arise from the initial and saddle-point π-electronic states near the K and M valleys, directly reflecting the main features of electronic energy spectra and wave functions {Fig. 1(b); [4]}. Furthermore, their van Hove singularities are strengthened and widened by the greatly enhanced interlayer van der Waals interactions [4]. There exist two strong peaks in valence/conduction density of states [not shown], or four obvious ones in the joint density of states during the vertical optical transitions. However, two/one transition channels are forbidden in the low-/middle-frequency electric-dipole excitations. This is responsible for the whole π-electronic optical excitations. It should be noticed that the dielectric functions become hardly independent of the sufficiently high layer numbers, e.g., those of $N_L \geq 50$ [Figs. 4(a) and 4(b)]. They account for the significant couplings between charges and waves and thus determine the diverse absorption, reflectance and transmittance behaviors.

The rich and unique optical properties deserve a closer examination, especially for cooperation or competition between π-electronic excitations and finite-width quantum confinement. Both $R(\omega)$ and $T(\omega)$ present the non-monotonous frequency dependences in the large-fluctuation forms. Such behaviors mainly come from the strong response functions under the prominent structures [the pronounced joint van Hove singularities]. As for the layer number of graphene systems, it provides more information about the decline of a propagating wave and its couplings with charges. Transmittance exhibits an obvious reduce in the increment of N_L. It is almost vanishing within the whole frequency range, while layer number is beyond 1000. Such results suggest a sufficiently high absorption coefficient [the observable imaginary part of dielectric functions]. On the other hand, reflectance might present the irregular/regular N_L-dependence at $\omega > 0.2$ eV/others. The unusual phenomena of $R(\omega)$ should be closely related to the magnitude of the dielectric

function. For example, $\epsilon\,(\omega\,)$ is about >100 and <10 at low and middle frequencies, respectively. Under the latter case, more optical scatterings would appear at two boundaries, being supported by the slow energy dissipation of the propagating electromagnetic waves. This might lead to the comparable $R(\omega\,)$s among the different layer numbers or the absence of the monotonic thickness dependence.

The current work clearly illustrates that charge screening abilities and boundary conditions play the critical roles in the rich and unique optical properties. Both mechanisms are very sensitive to the finite-size quantum effects. In general, any measured sample has a layered or non-planar structure, e.g., a sp^2 graphene or a sp^3 diamond with the upper and lower boundaries [Fig. 2]. Electronic properties and dielectric functions of the former are discussed in Eqs. (1) and (2). They could be calculated in the presence of perpendicular electric and magnetic fields, since the sublattice-based superposition is utilized in the generalized tight-binding model.

Also, the rich intrinsic interactions, which arise from the stacking symmetries [4], the multi-orbital hybridizations [38] and spin-orbital couplings [38], are included in the various Hamiltonians. Reflectance and transmittance spectra of few-layer graphene systems are thus expected to exhibit the diverse magnetic quantization phenomena under the various stacking configurations [38]. But when a bulk system gradually reduces its thickness, electronic energy spectra and wave functions will display a dramatic transform and thus dynamic charge responses. The width-created drastic changes of essential properties become an extra challenge. Such issue is worthy of the systematic investigations. Apparently, the current optical scatterings of layered materials has been covered in the theoretical development of quasiparticle framework [14]. That is, electronic, magnetic, optical, Coulomb-excitation and transport properties could be explored simultaneously from the modified and unified phenomenological models.

4 Conclusions

Optical scatterings are fully explored for layered materials under the theoretical framework of quasiparticles [14], being suitable for the rich and unique intrinsic interactions and the external fields. The fundamental properties are unified together and could be understood simultaneously. Specifically, layered graphene systems, with AB stackings, clearly show the unusual reflectance and transmittance spectra through the quantum-size effects. The strong frequency and thickness dependences illustrate the prominent π-electronic excitations and their significant couplings with electromagnetic waves.

Acknowledge

We would like to acknowledge the financial support from the Ministry of Science and Technology of the Republic of China (Taiwan) under Grant No. MOST 107-2112-M-017-001.

References

[1] Geim, A. K. & Novoselov, K. S. The rise of graphene. *Nature materials* **6**, 183 (2007)

[2] Castro Neto, A. H., Guinea, F., Peres, N. M. R., Novoselov, K. S. & Geim, A. K. The electronic properties of graphene. *Rev. mod. phys.* **81**, 109 (2009)

[3] Bae, S., Kim, H., Lee, Y., Xu, X., Park, J.-S., Zheng, Y., Balakrishnan, J., Lei, T., Kim, H. R., Song, Y. I., Kim, Y.-J., Kim, K. S., Özyilmaz, B., Ahn, J.-H., Hong, B. H. & Iijima, S. Roll-to-roll production of 30-inch graphene films for transparent electrodes. *Nat. nanotech.* **5**, 574 (2010)

[4] Lin, C. Y., Chen, R. B., Ho, Y. H. & Lin, M. F. Electronic and optical properties of graphite-related systems. *CRC Press*, Florida (2018)

[5] Ho, Y.-H., Chiu, Y.-H., Lin, D.-H., Chang, C.-P. & Lin, M.-F. Magneto-optical selection rules in bilayer bernal graphene. *ACS Nano* **4**, 1465–1472 (2010)

[6] Gusynin, V. P., Sharapov, S. G. & Carbotte, J. P. Anomalous absorption line in the magneto-optical response of graphene. *Phys. Rev. lett.* **98**, 157402 (2007)

[7] Abergel, D. S. L. & Fal'ko, Vladimir I. Optical and magneto-optical far-infrared properties of bilayer graphene. *Phys. Rev. B* **75**, 155430 (2007)

[8] Orlita, M., Faugeras, C., Plochocka, P., Neugebauer, P., Martinez, G., Maude, D. K., Barra, A.-L., Sprinkle, M., Berger, C., de Heer, W. A. & Potemski, M. Approaching the dirac point in high-mobility multilayer epitaxial graphene. *Phys. Rev. lett.* **101**, 267601 (2008)

[9] Mak, K. F., Shan, J. & Heinz, T. F. Electronic structure of few-layer graphene: experimental demonstration of strong dependence on stacking sequence. *Phys. Rev. lett.* **104**, 176404 (2010)

[10] Wang, F., Zhang, Y., Tian, C., Girit, C., Zettl, A., Crommie, M. & Shen, Y. R. Gate-variable optical transitions in graphene. *Science* **320**, 206 (2008)

[11] Sensale-Rodriguez, B., Yan, R., Rafique, S., Zhu, M., Li, W., Liang, X., Gundlach, D., Protasenko, V., Kelly, M. M., Jena, D., Liu, L. & Xing, H. G. Extraordinary control of terahertz beam reflectance in graphene electro-absorption modulators. *Nano lett.* **12**, 4518-4522 (2012)

[12] Skulason, H. S., Gaskell, P. E. & Szkopek, T. Optical reflection and transmission properties of exfoliated graphite from a graphene monolayer to several hundred graphene layers. *Nanotechnology* **21**, 295709 (2010)

[13] Novoselov, K. S., Geim, A. K., Morozov, S. V., Jiang, D., Katsnelson, M. I., Grigorieva, I. V., Dubonos, S. V. & Firsov, A. A. Two-dimensional gas of massless Dirac fermions in graphene. *Nano lett.* **438**, 197 (2005)

[14] Lin, C. Y., Wu, J. Y., Chiu, C. W. & Lin, M. F. Coulomb excitations and decays in graphene-related systems. *CRC Press*, Florida (2019)

[15] Wallace, P. R. The band theory of graphite. *Phys. Rev.* **71**, 622 (1946)

[16] Iijima S. & Ichihashi, T. Single-shell carbon nanotubes of 1-nm diameter. *Nature* **363**, 603 (1993)

[17] Odom, T. W., Huang, J.-L., Kim, P. & Lieber, C. M. Structure and electronic properties of carbon nanotubes. *J. Phys. Chem. B* **104**, 2794-2809 (2000)

[18] Saito, R., Fujita, M., Dresselhaus, G. & Dresselhaus, M. S. Electronic structure of chiral graphene tubules. *Appl. Phys. Lett.* **60**, 2204 (1992)

[19] Cai, J., Ruffieux, P., Jaafar, R., Bieri, M., Braun, T., Blankenburg, S., Muoth, M., Seitsonen, A. P., Saleh, M., Feng, X., Müllen, K. & Fasel, R. Atomically precise bottom-up fabrication of graphene nanoribbons. *Nature* **466**, 470 (2010)

[20] Nakada, K., Fujita, M., Dresselhaus, G. & Dresselhaus, M. S. Edge state in graphene ribbons: nanometer size effect and edge shape dependence. *Phys. Rev. B* **54**, 17954 (1996)

[21] Chung, H.-C., Chang, C.-P., Lin, C.-Y. & Lin, M.-F. Electronic and optical properties of graphene nanoribbons in external fields. *Phys. Chem. Chem. Phys.* **18**, 7573-7616 (2016)

[22] Pech, D., Brunet, M., Durou, H., Huang, P., Mochalin, V., Gogotsi, Y., Taberna, P.-L. & Simon, P. Ultrahigh-power micrometre-sized supercapacitors based on onion-like carbon. *Nat. nanotech.* **5**, 651 (2010)

[23] Tomita, S., Sakurai, T., Ohta, H., Fujii, M. & Hayashi, S. Structure and electronic properties of carbon onions. *J. Chem. Phys.* **114**, 7477 (2001)

[24] Kroto, H. W., Heath, J. R., O'Brien, S. C., Curl, R. F. & Smalley, R. E. C_{60}:Buckminsterfullerene. *Nature* **318**, 162 (1985)

[25] Lin, Y.-L. & Nori, F. Electronic structure of single- and multiple-shell carbon fullerenes. *Phys. Rev. B* **49**, 5020 (1994)

[26] Jackson, J. D. Classical electrodynamics. *Wiley*, New York (1975)

[27] Min, H. & MacDonald, A. H. Chiral decomposition in the electronic structure of graphene multilayers. *Phys. Rev. B* **77**, 155416 (2008)

[28] Lin, C.-Y., Wu, J.-Y., Ou, Y.-J., Chiu, Y.-H. & Lin, M.-F. Magneto-electronic properties of multilayer graphenes. *Phys. Chem. Chem. Phys.* **17**, 26008-26035 (2015)

[29] Charlier, J.-C., Michenaud, J.-P. & Lambin, Ph. Tight-binding density of electronic states of pregraphitic carbon. *Phys. Rev. B* **46**, 4540 (1992)

[30] Charlier, J.-C., Michenaud, J.-P. & Gonze, X. First-principles study of the electronic properties of simple hexagonal graphite. *Phys. Rev. B* **46**, 4531 (1992)

[31] Do, T.-N., Lin, C.-Y., Lin, Y.-P., Shih, P.-H. & Lin, M.-F. Configuration-enriched magneto-electronic spectra of AAB-stacked trilayer graphene. *Carbon* **94**, 619-632 (2015)

[32] Dressel, M. & Gruner, G. Electrodynamics of solids: optical properties of electrons in matter. *Cambridge University Press*, Cambridge (2002)

[33] Blinowski, J., Hy Hau, Nguyen, Rigaux, C., Vieren, J. P., Le Toullec, R., Furdin, G. & Melin, A. Hérold et J. Band structure model and dynamical dielectric function in lowest stages of graphite acceptor compounds. *J. Phys. France* **41**, 47-58 (1980)

[34] Lin, M. F. & Shung, Kenneth W.-K. Plasmons and optical properties of carbon nanotubes. *Phys. Rev. B* **50**, 17744 (1994)

[35] Chiu, C.-W., Chen, S.-C., Huang, Y.-C., Shyu, F.-L. & Lin, M.-F. Critical optical properties of AA-stacked multilayer graphenes. *Appl. Phys. Lett.* **103**, 041907 (2013)

[36] Chiu, C.-W., Ho, Y.-H., Shyu, F.-L. & Lin, M.-F. Layer-enriched optical spectra of AB-stacked multilayer graphene. *Appl. Phys. Express* **7**, 115102 (2014)

[37] Chiu, C.-W. & Chen, R.-B. Influence of electric fields on absorption spectra of AAB-stacked trilayer graphene. *Appl. Phys. Express* **9**, 065103 (2016)

[38] Lin, C. Y., Do, T. N., Wu, J. Y., Shih, P. H., Lin, S. Y., Ho, C. H. & Lin, M. F. Diverse quantization phenomena in emergent layered materials. *CRC Press*, Florida (2019)

[39] Xiao, S., Mei, H., Han, D., Dassios, K. G. & Cheng, L. Ultralight lamellar amorphous carbon foam nanostructured by SiC nanowires for tunable electromagnetic wave absorption. *Carbon* **122**, 718-725 (2017)

[40] Liu, X., Fan, K., Shadrivov, I. V. & Padilla, W. J. Experimental realization of a terahertz all-dielectric metasurface absorber. *Opt. Express* **25**, 281296 (2017)

Figure captions

Figure 1. A $N_L = 5$ AB-stacked graphene: (a) geometry with the significant atomic interactions and (b) 2D band structure, the inset shows the detail results.

Figure 2. Optical scatterings inside a finite-width sample.

Figure 3. (a) reflectance and (b) transmittance spectra for AB-stacked layered graphene systems with distinct layer numbers.

Figure 4. (a) The imaginary- and (b) real-part dielectric functions of AB-stacked graphene systems with layer numbers of 50 and 100.

Figures

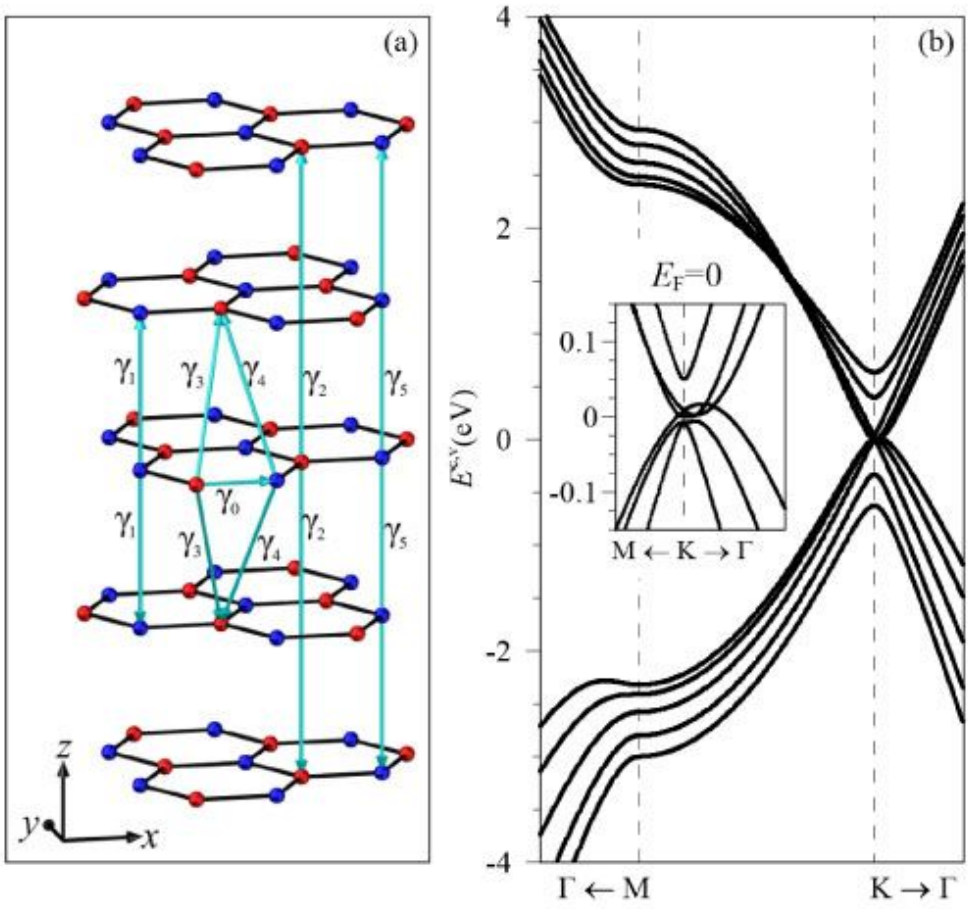

Figure 1

A NL = 5 AB-stacked graphene: (a) geometry with the signicant atomic interactions and (b) 2D band structure, the inset shows the detail results.

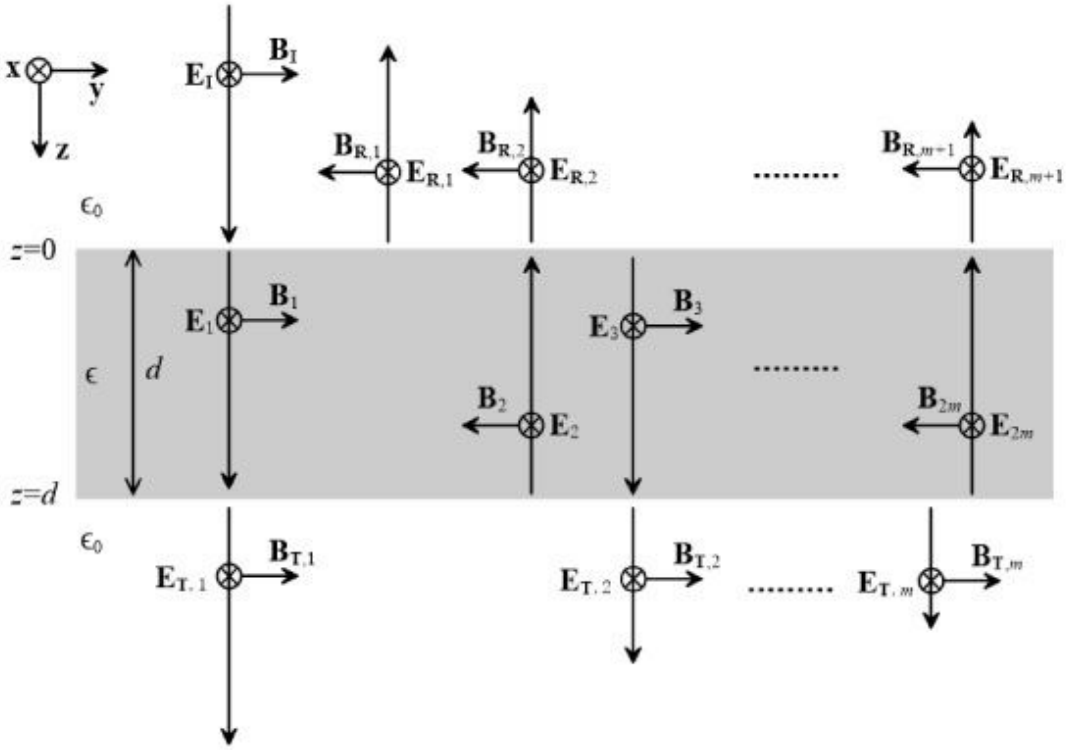

Figure 2

Optical scatterings inside a width sample.

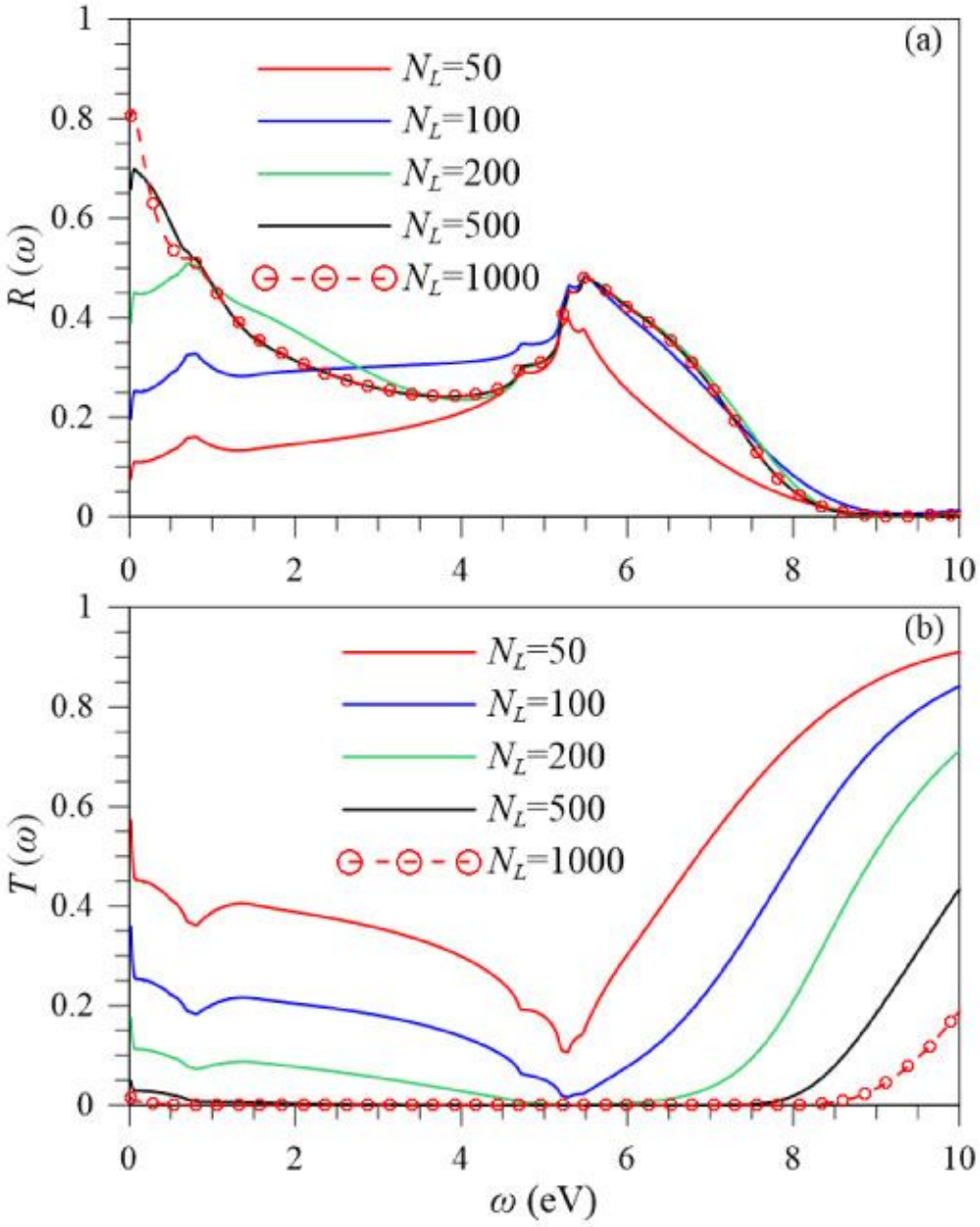

Figure 3

(a)reflectance and (b) transmittance spectra for AB-stacked layered graphene systems with distinct layer numbers.

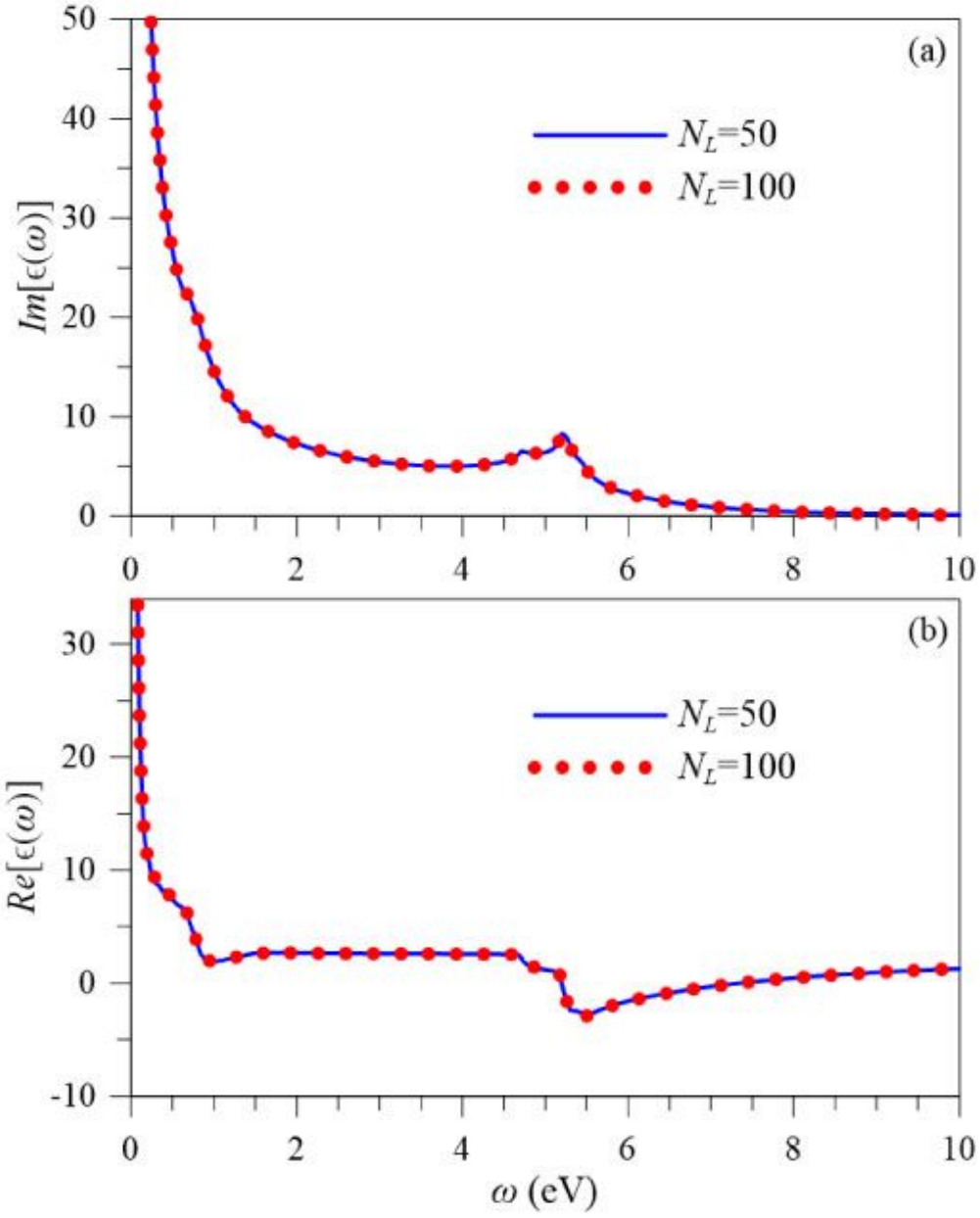

Figure 4

(a) The imaginary- and (b) real-part dielectric functions of AB-stacked graphene systems with layer numbers of 50 and 100.